Strength Analysis of Tubular Oil to Oil Cable Box Power Transformer GIS 60 MVA in the Case of Voltage Arc Energy Using the Finite Element Analysis Method

Asep Dharmanto[1], Asep Saepudin[1], Wilarso[1*]

[1] *Sekolah Tinggi Teknologi Muhammadiyah Cileungsi, Jl. Anggrek, No. 25, Perum PTSC, Cileungsi, Bogor, Jawa Barat-Indonesia 16820*

[*] *Email: wilarso@sttmcileungsi.ac.id*

Article Information:

Received:
26 August 2022

Received in revised form:
18 November 2022

Accepted:
15 December 2022

Volume 4, Issue 2, December 2022
pp. 55 – 60

https://doi.org/10.23960/jesr.v4i2.110

Abstract

The power transformer is an essential part of the electrical distribution system because it must be reliable and safe from fire and explosions, one of which is brought on by internal oil arching that results in overheating. In general, on the high voltage side of the transformer, there are power transformers fitted with tubular oil to oil cable boxes for the demands of the client. The tubular oil to oil cable box is installed to reduce space in substations with limited space as well as to boost safety against weather and pollution at the high voltage terminal section of power transformers. The goal of this investigation is to determine the cause of an explosion that occurred in a tubular oil-to-oil cable box on the high voltage side of a Gas Insulation System (GIS) type power transformer with a power of 60 MVA and a voltage rating of 150/20 kV. For all parties involved, this incident will serve as a lesson about what to avoid doing in the future with similar power transformers. In this study, we will use a qualitative method with Finite Element Analysis (FEA), which takes samples and data of a Gas Insulation System (GIS) power transformer on the high voltage side, especially in the analysis of tubular strength. This power transformer has a voltage rating of 150/20 kV and a power of 60 MVA. Applying normal pressure to a pressure that could harm the tubular oil to oil cable box can prevent damage. The tubular oil to oil cable box is built of SS400 material and has an 8mm thickness so that it can be determined how robust it is.

Keywords: *Internal Arcing*, *Short Circuit*, Tubular, GIS, FEA.

I. INTRODUCTION

There are various different types of bushings used in power transformers [1] and they can be roughly split into two groups: Non Condenser (Bulk) for use up to 72 kV and Condenser. According to the type of insulation used—Oil-impregnated paper, resin-impregnated paper, and resin-impregnated silicon. And based on their placement, they are divided into three types, namely in open air, in oil and in SF6 gas [2].

For the placement of the bushing in the oil and in the gas, SF6 generally uses a tubular. Figure 1 illustrates a GIS type power transformer on the high voltage side and in Figure 2 illustrates the details of tubular oil for HV

bushings.

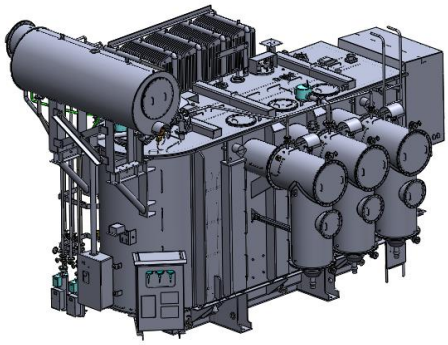

Figure 1. GIS power transformer

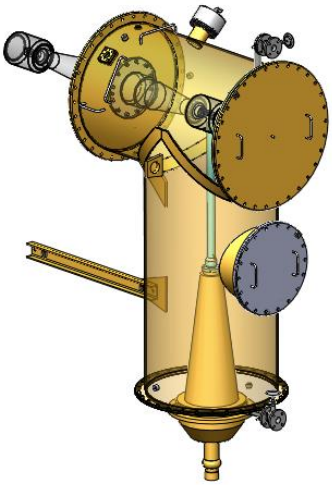

Figure 2. HV tubular oil bushing details

Due to the action of a short circuit, the internal arc in an oil-immersed transformer will result in high temperatures in the arc gas and the surrounding oil [3], but won't ignite a fire within the tank if oxygen is not available. Oil with dissolved oxygen cannot ignite a fire [4]. If the high-energy arc from the overcurrent breaks fast, the tank may burst and the high-temperature transformer oil may come into contact with metal at a temperature high enough to ignite it or the air may come into contact with metal and ignite the oil (fire triangle theory) [5].

Power transformers could still malfunction despite a multitude of electro-protection tools to avoid internal arc [6][7], These incidents happen anywhere from 1% to 1% of the time over a year. The internal arch instance causes a very big loss owing to damage to the transformer and environmental harm from fires that may be lethal.

As seen in **Figure 2**, tubular transformer failures that explode and subsequently catch fire will be examined in this essay. On the high voltage side of a Gas Insulation System (GIS) type power transformer with a power of 60 MVA and a voltage rating of 150/20 kV using SS400 material and 8 mm thick, precise analysis of the occurrence of disturbances in the tubular oil to oil cable box was obtained from PT X as manufacture and PT Y as user, then utilized a straightforward model. The data from the calculation of the pressure in the tube is then analyzed using the FEA analysis tool in SolidWorks. A tubular oil HV bushing that caught fire as a result of a short circuit is shown in **Figure 3**. The aim of this study to analyze the strength of tubular construction and to determine the cause of an explosion

Figure 3. Shows an oil-to-oil cable box with tubular bushing that caught fire and detonated.

II. MATERIALS AND METHODS

A. Materials

1. The materials used in this case study investigation are:
2. A power transformer of the GIS type with a power of 30/60 MVA and a voltage of 150/20 kV
3. Tubular Oil HV Bushing made from SS400 sheet steel
4. DELL Precision Series 3560. Laptop 4. Dassault Systemes France's Cosmosworks-Solidworks software

B. Methods

This study used a FEA (Finite Element Analysis) methodology using Dassault Systemses France's Cosmosworks-Solidworks software, with a meshing model size of 22 mm in the High category. The overall deviation size of a mesh element with an aspect ratio (number of sides of equal length) less than 3 is 75%. Two applications of the pressure analysis were made in tubular, with the first employing a pressure of 100 kPa (14.5 Psi) and the second using 500 kPa (72.5 psi). **Figure 4** depicts the analytical flowchart that is attached. It is the methodology used in the research, which starts with gathering field data and moves on to modeling, analyzing, and calculating tubular while being consistent with previously collected experimental data.

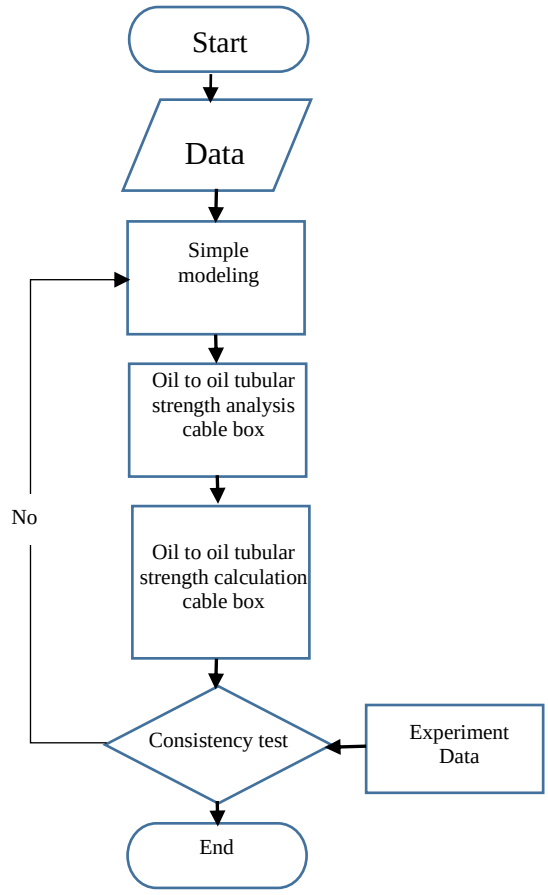

Figure 4. Flowchart of research design.

III. RESULTS AND DISCUSSIONS

A. Internal arc developing in the bushing conductor HV

Widespread overheating in the transformer can be brought on by an excessive current flowing through the wires, terminals, and transformer windings [8]. When there is electrical protection due to overpressure in the tubular space, it normally cuts off the current independently to prevent the continuation of overpressure and fire. If there is no oxygen, it does not produce a fire in the transformer tank.

The fault current data in phase R of 12 kA that is read on the differential relay 2 supports the theory that the fire may have originated with a short circuit from the 150 kV side to ground/tank without going through the winding transformer [9], Based on observations made in the field, a short circuit may originate from the sealing end phase R's bottom to the ground/tubular tank 3. This short circuit energy causes explosions, heat, and fire inside the tubular, which destroys the top flange of the tubular phase R and frees the OPRD phase R from the tubular as well as the flange's sealing end at the bottom of phase R.

Phase R's tubular flange was discovered to be deforming and bulging. Because heated oil exits the tubular phase R and comes into touch with the air, the fire is growing increasingly large (filled with the fire triangle). When oil was found to be leaking through the top flange of the tubular phase R, the first fire was discovered there. According to CIGRE 537-June 2013 [9], the energy formulation is as follows:

$$E_t = \int_0^{tarc} v.(t).i.(t).dt \quad (1)$$

E = *Vault energy*
v = *Arc Voltage*
i = *Arc current*

Data on voltage (v) and current are available during the t_{arch} period, which is the time frame in which a short circuit level occurs (i).$P_s =$

$$F\left[\ 100\sqrt{\frac{1}{4}+\frac{kE}{100C}}-50\ \right] \quad (2)$$

P_S = *Tank design pressure (kPa);*
E = *Fault energy level (kJ);*
k = *Arc energy conversion factor (5.8 × 10−4 m3/kJ) (@ 2000 K);*
C = *Tank expansion coefficient (2,024m^3/kPa);*
F = *Dynamic amplification factor (1,5-2,5);*

The data in the calculation in the table below uses a Varc of 45 kV and Iarc uses 12.8 kA as to be gained from recorded data substation. Table 1 describes the length of time that occurred and the amount of energy and pressure that appeared in the tubular oil to oil HV cable box until a fire and explosion occurred.

Table 1. Results of the calculation period for energy and pressure in the tubular

Period (t)	**Sec**	**0,071**	**0,55**	**0,7**
Energy (E_t)	**kJ**	1,57E+02	7,32E+04	1,51E+05
Pressure (Ps)	**kPa**	9,92E-02	3,92E+01	7,17E+01
Period (t)	**Sec**	**0,8**	**0,9**	**1**
Energy (E_t)	**kJ**	2,25E+05	3,21E+05	4,40E+05
Pressure (Ps)	**kPa**	9,82E+01	1,28E+02	1,60E+02
Period (t)	**Sec**	**1,1**	**1,2**	**1,3**
Energy (E_t)	**kJ**	5,86E+05	7,60E+05	9,67E+05
Pressure (Ps)	**kPa**	1,95E+02	2,33E+02	2,72E+02
Period (t)	**Sec**	**1,4**	**1,5**	**1,8**
Energy (E_t)	**kJ**	1,21E+06	1,49E+06	2,57E+06
Pressure (Ps)	**kPa**	3,14E+02	3,57E+02	4,97E+02
Period (t)	**Sec**	**2**	**2,7**	
Energy (E_t)	**kJ**	3,52E+06	8,66E+06	
Pressure (Ps)	**kPa**	5,97E+02	9,91E+02	

B. Protection system on tubular HV

Pressure Relieve Device protection with product code PRD 206 is used to safeguard the internal pressure

system in the tubular. When the tool is set at a pressure of 40 kPa with a plus-minus 7 kPa tolerance, it will function at pressures between 33 and 47 kPa in the tube. Alternatively, it takes 2 ms to achieve the operating pressure (trip) with a rise of 28 kPa.

C. Strength of HV tubular construction.

The strength of the tubular itself is estimated [10], after the energy, internal pressure in the current-carrying system, and pressure protection in the tubular have been computed [11]. Finite element analysis (FEA) was used to analyze the tubular construction's strength [12] using Cosmosworks-Solidworks software from Dassault Systemes France [13].

The following describes the HV tubular bushing's precise geometry as seen through a 3-dimensional software visualization:

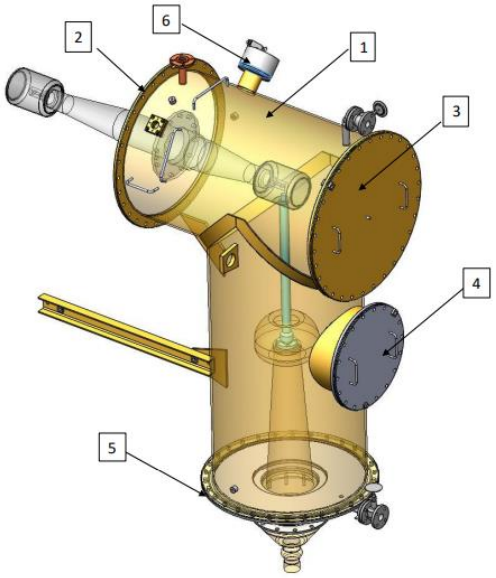

Figure 5. Tubular bushing HV

Figure 5 provides a thorough explanation of the tubular oil HV bushing by listing the components.

The following materials are used in the tubular construction:

1. An 8 mm thick, tubular main tube made of S400.
2. The entire flange is made of 304L stainless steel with a thickness of 16 mm.
3. The manhole cover is made of S400 material and is 10 mm thick.
4. The middle manhole cover is made of S400 material and is 10 mm thick.
5. The bottom end seal cover is made of S400 material and is 15 mm thick.
6. PRD construction made of aluminum.

All plates used in 3D modeling include material requirements and are made of S400. The maximum permissible strength is 160 MPa, the yield strength is 220 MPa, and the ultimate strength is 370 MPa. The portion of the model that is fastened to the transformer's wall is known as the fixed mounted. Model meshing employs a size of 22 mm with a High category [14][15]. The overall deviation size of a mesh element with an aspect ratio (number of sides of equal length) less than 3 is 75%. Two applications of pressure analysis in the tubular were made: one at a pressure of 100 kPa (14.5 Psi) and the other at a pressure of 500 kPa (72.5 psi). Following the FEA, the results are as follows:

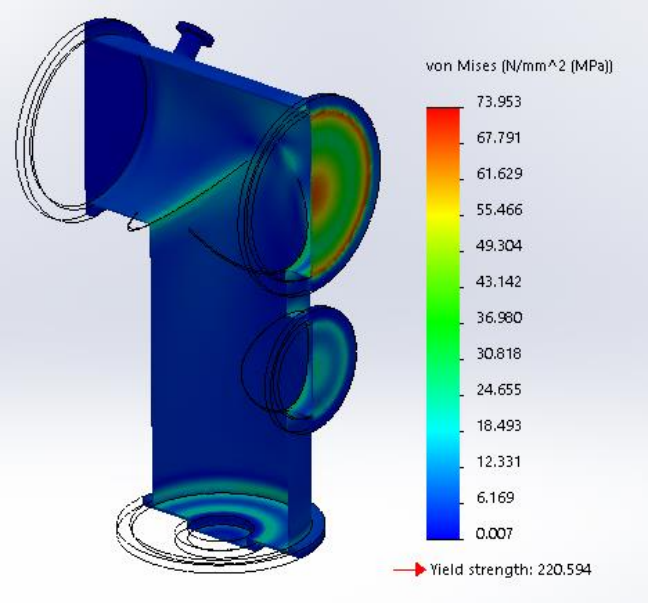

Figure 6. The stress that occurs is the result of an internal pressure of 100 kPa.

Inputting a pressure of 100 kPa and a stress of 73.9 MPa on the upper flange—where the material's strength has a stress limit of 160 MPa—results in **Figure 6**. Because the peak stress in this situation occurs at a value of 73.9 MPa, which is still much below the acceptable limit of 160 MPa (Allowable Strength) [13]., the tubular construction is still considered to be safe and not in failure state.

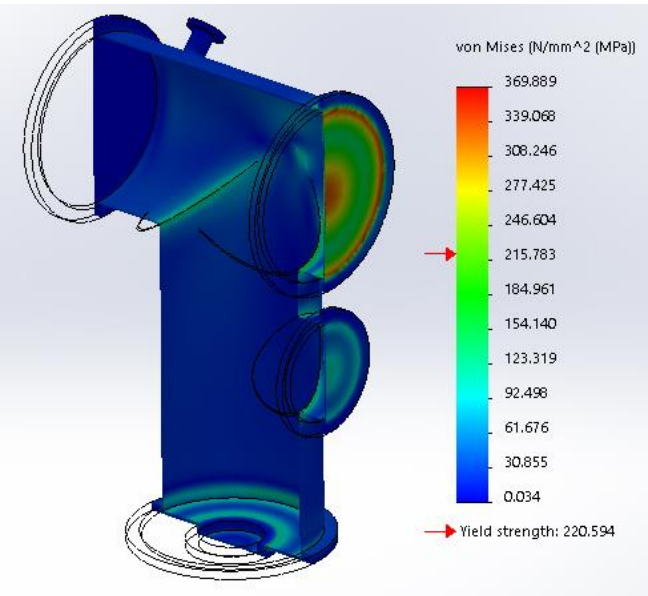

Figure 7. Shows the stress that results from 500 kPa of internal pressure.

In general transformer tanks are designed to withstand an internal operating pressure of approximately 50-100 kPa (relative to Atmospheric and above head of oil), and to withstand full vacuum without plastic deformation. Therefore, the ultimate rupture pressure can be evaluated somewhat above 150-200 kPa. It is the working groups experience that tanks for large HV transformers >100 MVA, typically have flexibility in the range of 0.5 -1.5 % volume expansion per 100 kPa pressure increase [9]. Figure 7 shows the simulation's outcome when a pressure of 500 kPa and a stress of 369.8 MPa are applied to the upper flange. The material's maximum stress before fracture is 370 MPa, and according to Table 1. the simulation's pressure of 500 kPa occurs within 1.8 seconds. In this instance, the highest stress occurs at a value of 369.8 MPa, which is the same value as the fracture limit of 370 MPa, causing damage to the tubular construction due to peak elongation (Ultimate Strength) [16]

IV. CONCLUSIONS

Based on study results from tubular FEA performed safely at 100 kPa of pressure. If there is internal pressure up to 500 kPa, the tubular will rupture. According to Table 1, the pressure development period is 0.8 seconds for pressures up to 100 kPa and 1.8 seconds for pressures up to 500 kPa. The pressure protection mechanism operates between 33 and 47 kPa for 0.55 seconds. The protective mechanism should be able to function and stop the short circuit in around 0.55 seconds with a response speed of 0.002 seconds. This data search reveals that the tube detonated as a result of the protection system failing to activate in the presence of a short circuit current.

ACKNOWLEDGMENT

Thank you to the Muhammadiyah Cileungsi College of Technology for funding the research conducted by the lecturers.

REFERENCES

[1] J. Li, Z. Li, J. Chen, Y. Bie, J. Jiang, and X. Yang, "Oil pressure monitoring for sealing failure detection and diagnosis of power transformer bushing," *Energies*, vol. 14, no. 23, 2021, doi: 10.3390/en14237908.

[2] L. Gong and S. Zhang, "Application of combined gas chromatography and dielectric spectroscopy in SF6 gas insulated high voltage converter transformer bushing insulation performance," *J. Phys. Conf. Ser.*, vol. 1748, no. 5, 2021, doi: 10.1088/1742-6596/1748/5/052013.

[3] C. Yan, Z. Hao, S. Zhang, B. Zhang, and T. Zheng, "Numerical methods for the analysis of power transformer tank deformation and rupture due to internal arcing faults," *PLoS One*, vol. 10, no. 7, 2015, doi: 10.1371/journal.pone.0133851.

[4] DVN GL SE Germanischer Lloyd SE, "Rules for classification and construction – ship technology - Underwater Technology - Manned Submersibles," no. January, pp. 1–156, 2016.

[5] G. Perigaud, S. Muller, G. De Bressy, R. Brady, and P. Magnier, "an Answer To Prevent Transformer Explosion and Fire : Live Test and Simulations on," pp. 1–14, 2008.

[6] Y. Xia, Z. Shi, Y. Li, Y. Feng, and Z. Xu, "Dynamic Analysis and Control Measures of Distribution Network Voltage with Electric Arc Furnace," 2019, doi: 10.1109/ICPDS47662.2019.9017177.

[7] Y. Hu, Z. Chen, Z. Chen, and Y. Yuan, "A new method for analyzing the influence of the impact load in steel plant on grid," 2011, doi: 10.1109/DRPT.2011.5993896.

[8] Y. Goda, M. Iwata, K. Ikeda, and S. I. Tanaka, "Arc voltage characteristics of high current fault arcs in long gaps," *IEEE Trans. Power Deliv.*, vol. 15, no. 2, 2000, doi: 10.1109/61.853021.

[9] A. Petersen *et al.*, "Guide for transformer fire safety practices," *Electra*, vol. 268, no. June, pp. 43–49, 2013.

[10] Y. Han and Y. Bao, "Analysis on Seismic Performance of Steel-Reinforced Concrete-Filled Circular Steel Tubular (SRCFST) Members Subjected to Post-Fire," *Materials (Basel).*, vol. 15, no. 6, 2022, doi: 10.3390/ma15062294.

[11] Y. L. Huibin Sun, Wei Lu, Jiancai Wang, Quangang Ren, Xin Xu, Debin Han, Xu Li, Huixiang Yang, Lianbang Wei, "Comparative Study on Compressive and Flexural Properties of Concrete-Filled Steel Tubular Arch Joints," *Sustainability*, vol. 14, no. 8916, 2022, doi: DOI: 10.3390/su14148916.

[12] T. Xu, K. Wang, and S. Song, "Measurement uncertainty and representation of tensile mechanical properties in metals," *Metals*, vol. 11, no. 11. 2021, doi: 10.3390/met11111733.

[13] S. Brodeur, V. N. Lê, and H. Champliaud, "A nonlinear finite-element analysis tool to prevent rupture of power transformer tank," *Sustain.*, vol. 13, no. 3, 2021, doi: 10.3390/SU13031048.

[14] K. Woloszyk and Y. Garbatov, "An enhanced method in predicting tensile behaviour of corroded thick steel plate specimens by using random field approach," *Ocean Eng.*, vol. 213, 2020, doi: 10.1016/j.oceaneng.2020.107803.

[15] S. Zeng, S. Gu, S. Ren, Y. Gu, C. Kong, and L. Yang, "A Modeling Method for Finite Element Analysis of Corroded Steel Structures with Random Pitting Damage," 2022.

[16] H. X. Yueqi Bi, Xiaoming Yuan, Mingrui Hao,

Shuai Wang, "Numerical Investigation of the Influence of Ultimate-Strength Heterogeneity on Crack Propagation and Fracture Toughness in Welded Joints," *Materials (Basel).*, vol. 15 (11), no. 3814, 2022, doi: DOI: 10.3390/ma15113814.